# Significant increase of summertime ozone at Mount Tai in Central Eastern China

Lei Sun[1], Likun Xue[1*], Tao Wang[2,1], Jian Gao[3], Aijun Ding[4], Owen R. Cooper[5,6], Meiyun Lin[7,8], Pengju Xu[9], Zhe Wang[2], Xinfeng Wang[1], Liang Wen[1], Yanhong Zhu[1], Tianshu Chen[1], Lingxiao Yang[1,10], Yan Wang[10], Jianmin Chen[1,10], Wenxing Wang[1]

[1] Environment Research Institute, Shandong University, Ji'nan, Shandong, China

[2] Department of Civil and Environmental Engineering, Hong Kong Polytechnic University, Hong Kong, China

[3] Chinese Research Academy of Environmental Sciences, Beijing, China

[4] Institute for Climate and Global Change Research and School of Atmospheric Sciences, Nanjing University, Nanjing, Jiangsu, China

[5] Cooperative Institute for Research in Environmental Sciences, University of Colorado, Boulder, Colorado, USA

[6] NOAA Earth System Research Laboratory, Boulder, Colorado, USA

[7]Atmospheric and Oceanic Sciences, Princeton University, Princeton, New Jersey, USA

[8] NOAA Geophysical Fluid Dynamics Laboratory, Princeton, New Jersey, USA

[9] School of Geography and Environment, Shandong Normal University, Ji'nan, Shandong, China

[10] School of Environmental Science and Engineering, Shandong University, Ji'nan, Shandong, China

*To whom correspondence should be addressed: Likun Xue: xuelikun@sdu.edu.cn

**Abstract.**

Tropospheric ozone ($O_3$) is a trace gas playing important roles in atmospheric chemistry, air quality and climate change. In contrast to North America and Europe, long-term measurements of surface $O_3$ are very limited in China. We compile available $O_3$ observations at Mt. Tai – the highest mountain over the North China Plain – during 2003-2015 and analyze the decadal change of $O_3$ and its sources. A

linear regression analysis shows that summertime $O_3$ measured at Mt. Tai has increased significantly by 1.7 ppbv $yr^{-1}$ for June and 2.1 ppbv $yr^{-1}$ for the July–August average. The observed increase is supported by a global chemistry-climate model hindcast (GFDL-AM3) with $O_3$ precursor emissions varying from year to year over 1980-2014. Analysis of satellite data indicates that the $O_3$ increase was mainly due to the increased emissions of $O_3$ precursors, in particular volatile organic compounds (VOCs). An important finding is that the emissions of nitrogen oxides ($NO_x$) have diminished since 2011, but the increase of VOCs appears to have enhanced the ozone production efficiency and contributed to the observed $O_3$ increase in central eastern China. We present evidence that controlling $NO_x$ alone, in the absence of VOC controls, is not sufficient to reduce regional $O_3$ levels in North China in a short period.

## 1. Introduction

Ozone ($O_3$) in the troposphere is a trace gas of great importance for climate and air quality. It is the principal precursor of the hydroxyl radical (OH) which plays a central role in atmospheric chemistry (Seinfeld and Pandis, 2006), and the third most important greenhouse gas contributing to the warming of the Earth (IPCC, 2013). At ground level, high levels of $O_3$ have adverse effects on human health and ecosystem productivity (National Research Council, 1991; Monks et al., 2015). In the troposphere, the ambient $O_3$ burden is the product of the flux from the stratosphere (e.g., Stohl et al., 2003; Lin M. et al., 2015a), dry deposition, and net photochemical production involving the reactions of nitrogen oxides ($NO_x$) with carbon monoxide (CO) and volatile organic compounds (VOCs) in the presence of sunlight (Crutzen, 1973; Ma et al., 2002). Increases in anthropogenic emissions of ozone precursors have contributed to changes in the tropospheric $O_3$ abundances, both globally and regionally (The Royal Society, 2008; Cooper et al., 2014; Monks et al., 2015; Lin M. et al., 2015b). Decadal shifts in climate and circulation regimes can also contribute to changes in tropospheric $O_3$, as found in the 40-year record at Mauna Loa Observatory in Hawaii (Lin M. et al., 2014). Conversely, the changes in tropospheric $O_3$ may also pose significant feedbacks to the environment and climate (e.g., Shindell et al, 2012; Stevenson et al, 2013). Therefore, the long-term changes (or trends) of tropospheric $O_3$ has long been a topic of great interest in the atmospheric sciences.

Since the 1970s, long-term measurements of surface $O_3$ (and $O_3$ precursors) have been increasingly carried out worldwide, mostly in North America and Europe (e.g., Logan et al., 2012; Oltmans et al., 2013; Cooper et al., 2014). The existing knowledge of tropospheric $O_3$ trends has been recently reviewed (UNEP, 2011; Cooper et al., 2014; Monks et al., 2015). Overall, upward trends have been recorded around the world since the 1970s, but trends over the past two decades have varied regionally. In Europe, the surface $O_3$ in rural or remote areas, usually regarded as the regional baseline $O_3$, rose until the year 2000 but has since leveled off or decreased (Logan et al., 2012; Oltmans et al., 2013; Parrish et al., 2012). In the eastern US, summertime $O_3$ at most rural and urban stations has decreased over 1990–2010 (Lefohn et al., 2010; Cooper et al., 2012). In the western US, extreme ozone events have decreased in urban areas, particularly in southern California (Warneke et al., 2012), but springtime $O_3$ at remote mountain sites has shown large interannual variability due to stratospheric influence (Lin M. et al., 2015a), with little overall trends or small increases (Cooper et al., 2012; Fine et al., 2015). Analysis of available observations and chemistry-climate model hindcast indicates that springtime $O_3$ in the free troposphere over western North America has increased significantly by 0.4 ppbv $yr^{-1}$ over 1995-2014 (Lin M. et al., 2015b).

In comparison with North America and Europe, investigations of long-term $O_3$ trends are scarce in China, where rapid urbanization and industrialization has occurred over the past three decades. Significant increasing trends of surface $O_3$ have been derived from a handful of long-term monitoring stations over China, including Beijing (Tang et al., 2009; Zhang et al., 2014), Hong Kong (Xue et al., 2014), Taiwan (Lin et al., 2010) and Mount Waligian (Xu et al., 2016). Based on the MOZAIC commercial aircraft measurements, Ding et al. (2008) derived an $O_3$ increase of ~2% per year from 1995 to 2005 for the lower troposphere above Beijing by analyzing the difference between observations from 1995–2000 and 2000–2005. Wang et al. (2009) reported the first long-term continuous observations of Chinese surface $O_3$ at a regional background site in southern China (Hok Tsui), and indicated an average increase of 0.58 ppbv $yr^{-1}$ during 1994–2007. Xu et al. (2016) recently reported another continuous $O_3$ record (1994–2013) at Mt. Waliguan, a Global Atmospheric Watch station in western China, and found significant positive trends with 0.15–0.27 ppbv $yr^{-1}$ for daytime $O_3$ and

0.13–0.29 ppbv $yr^{-1}$ for nighttime $O_3$. Despite the valuable information obtained from the abovementioned efforts, additional studies are required to improve our understanding of tropospheric $O_3$ trends across the rapidly developing China. In particular, long-term observations covering more than ten years remain very limited over the highly polluted regions of central eastern China.

In recent years, China has implemented a series of stringent air quality control measures. Following the successful reductions in sulfur dioxide ($SO_2$) emissions since 2006 (Lu et al., 2010), China has recently launched a national programme to reduce $NO_x$ emissions during its "Twelfth Five-Year Plan" (2011–2015) (China State Council, 2011). However, to our knowledge, fewer controls have been placed on VOC emissions in China. Rather, anthropogenic VOC emissions have continued to increase (Bo et al., 2008; Wang et al., 2014). Therefore, it is of great interest and critical importance to evaluate the effect of the current control policy (i.e., controlling $NO_x$ with little action for VOCs) on regional $O_3$ and other secondary air pollution problems in China.

Mt. Tai (36.25 °N, 117.10 °E; 1534 m altitude) is the highest mountain in the center of the North China Plain (NCP; see Fig. 1) – a fast developing region facing severe air pollution. During daytime, the summit is well within the planetary boundary layer (PBL), and the site is therefore regionally representative of the region (Kanaya et al., 2013). Since 2003, several field measurement campaigns have been conducted at this site, with surface $O_3$ of major interest. In this paper, we analyze all available $O_3$ and its precursor observations at Mt. Tai to understand the summertime $O_3$ characteristics, including trends. To place the short observational record into a long-term context, we analyze multi-decadal hindcast simulations (1980-2014) conducted with the GFDL-AM3 chemistry-climate model (Lin M. et al., 2014; 2015a, b). In the following sections, we first present the seasonal and diurnal ozone variations followed by the climatological air mass transport pattern in summer. We then derive the $O_3$ trend (or systematic change) during 2003–2015 using linear regression. We finally elucidate the key factors affecting the $O_3$ trends by examining satellite and in-situ observed trace gas data. Our analysis demonstrates a significant increase of summertime surface $O_3$ at this important regional site in northern China, and indicates the urgent need of VOC control in China to reduce regional $O_3$ pollution.

## 2. Observational data set

The observations analyzed in the present study are summarized in Table 1. It comprises several sets of field observations from different periods. The earliest $O_3$ measurements at Mt. Tai were made from July–November 2003 (Gao et al., 2005), and the longest observations lasted for three years from June 2006 to June 2009 (despite a data gap in January–February 2007 owing to instrument maintenance). In recent years, we conducted intensive measurements at Mt. Tai during June–August of 2014 and 2015. In addition, another set of 3-year measurements was carried out from March 2004 to May 2007, as an international joint effort between Japanese and Chinese scientists (Kanaya et al., 2013); monthly average $O_3$ data are taken from this work. As most of the measurements are available for the period of June–August each year, we focus on the summertime $O_3$ in this study.

Two study sites have been used for field observations at Mt. Tai. One was the Mt. Tai Meteorological Observatory (Site 1) at the summit with an altitude of 1534 *m* a.s.l., and the other was in a hotel (Site 2) that is ~1 *km* to the northwest of Site 1 and slightly lower (1465 *m* a.s.l.; see *Fig. S1* for the site locations). Such elevations position these sites either within the PBL in the afternoon in summer, or in the free troposphere during the night. Although Mt. Tai is a famous tourism spot, both sites are located in the less frequently visited zones. Hence the impact of local anthropogenic emission should be small, and the data collected are believed to be regionally representative. Details of these sites have been described elsewhere (Site 1: Gao et al., 2005; Kanaya et al., 2013; Site 2: Guo et al., 2012; Shen et al., 2012). For our data set, most of the measurements were taken at Site 1, and only the intensive campaign in 2014 took place at Site 2.

All measurements were implemented using standard techniques, which were detailed in the previous publications (e.g., Gao et al., 2005; Xue et al., 2011). Briefly, $O_3$ was measured using a commercial ultraviolet photometric instrument (*Thermo Environment Instruments (TEI), Model 49C*) with a detection limit of 2 ppbv and a precision of 2 ppbv. CO was monitored with a gas filter correlation, non-dispersive infrared analyzer (*Teledyne Advanced Pollution Instrumentation, Model 300E*), with automatic zeroing every two hours. This technique has a detection limit of 30 ppbv and a

precision of 1% for a level of 500 ppbv. NO and $NO_2$* were measured by a chemiluminescence analyzer equipped with an internal MoO catalytic converter (*TEI, Model 42C*), with a detection limit of 0.4 ppbv and precision of 0.4 ppbv. Inter-comparison with a highly selective photolytic $NO_2$ detection approach indicated that the $NO_2$* measured with MoO conversion significantly overestimated $NO_2$ (i.e., up to 130% in afternoon hours), and $NO_2$* actually represented a major fraction (60%–80%) of $NO_y$ at Mt. Tai (Xu et al., 2013). During the measurements, the $O_3$ analyzer was calibrated routinely (i.e., quarterly for the 3-year observations in 2006–2009, and before and after the other campaigns) by an ozone primary standard (*TEI, Model 49PS*). For CO and $NO_x$*, zero and span calibrations were performed weekly during 2006–2009 and every three days during the intensive campaigns. Meteorological data including temperature, relative humidity (RH), and wind vectors were obtained from the Mt. Tai Meteorological Observatory, where Site 1 is located.

It is noteworthy that some portion of this long-term data set has been reported previously. Gao et al. (2005) analyzed the measurements of $O_3$ and CO from July–November 2003 and examined their diurnal variations and relations to backward trajectories. Kanaya et al. (2013) reported the observations in 2004–2007 and examined the processes influencing the seasonal variations and regional pollution episode. The major objective of the present study is to compile all of the available $O_3$-related observations at Mt. Tai and to establish the trend (or systematic change), if any, of ambient $O_3$ levels in the past decade at this unique site, regionally representative of the North China Plain.

## 3. Results and discussion

### 3.1. Seasonal and diurnal variations from more recent data

Figure 2 depicts the seasonal variation of surface $O_3$ at Mt. Tai derived from the more recent year-round observations from 2006–2009. Overall, $O_3$ shows higher levels in the warm season, i.e. April–October, compared to the cold season, i.e. November–March, with two peaks in June and October. The elevated $O_3$ levels in April and May should be affected by the stratosphere-troposphere exchange process which usually occurs at its maximum in the spring season (Yamaji et al., 2006). In addition to the high temperatures and intense solar radiation (especially in June), biomass burning is believed to be

another factor shaping the $O_3$ maximums in June and October, both of which are major harvest seasons of wheat and corn in northern China. The significant impacts of biomass burning on air quality over the North China Plain during June have been evaluated by a number of studies (Lin M. et al., 2009; Yamaji et al., 2010; Suthawaree et al., 2010). It is also noticeable that the $O_3$ concentrations in July and August at Mt. Tai are substantially lower than those in June. This is attributed in part to the more humid weather and greater precipitation in July and August in this region (see Table 2 for the RH condition). Inspection of meteorological conditions day by day also indicates a frequency of cloudy days (i.e., with RH $\geq$ 95%) of ~25% in June and of ~51% during July–August. In the following analyses, therefore, we assess the ozone characteristics separately for June and July–August.

Shown in the upper panel of Fig. 2 is the frequency of the maximum daily 8-hour average $O_3$ mixing ratios (MDA8 $O_3$) exceeding the 75-ppbv National Ambient Air Quality Standard (Class II). Although located in a relatively remote mountain-top area, the observed $O_3$ pollution at Mt. Tai was rather serious in the warm season, with frequencies of the $O_3$-exceedence days of over 45% throughout April–October. In particular, the occurrence of $O_3$-exceedence days was as high as 89% in June. These results demonstrate the severe $O_3$ pollution situation across the North China Plain.

Figure 3 illustrates the well-defined diurnal variations of surface $O_3$ with a trough in the early morning and a broad peak lasting from afternoon to early evening, which is commonly observed at polluted rural sites. As the summit of Mt. Tai is well above the PBL at nighttime, the $O_3$ concentrations during the latter part of the night (e.g., 2:00–5:00 LT) are usually considered to reflect the regional baseline $O_3$ (defined hereafter as regional $O_3$ without impact of local photochemical formation). Comparing the diurnal profiles in June and July–August clearly reveals the significantly higher regional baseline $O_3$ in June (with a mean difference of ~17 ppbv). On the other hand, the daytime $O_3$ build-up, defined as the increase in $O_3$ concentrations from the early-morning minimum to the late-afternoon maximum, may reflect the potential of regional $O_3$ formation. For the Mt. Tai case, the average daytime $O_3$ build-up was 22 ppbv in June and 15 ppbv in July–August, indicating the stronger photochemical ozone production in June. Hence, the more intense photochemistry and higher regional baseline bring about the more serious $O_3$ pollution in June at Mt. Tai.

Another remarkable feature of surface $O_3$ at Mt. Tai is the relatively high nighttime levels, with average concentrations of 75–85 ppbv in June and 60–70 ppbv during July–August. This should be the composite result of the residual $O_3$ produced in the preceding afternoon in the boundary layer, less $O_3$ loss from NO titration, and long-range transport of processed regional plumes. The transport of regional plumes was evidenced by the coincident evening $NO_2$* (including $NO_2$ and some higher oxidized nitrogen compounds) maximums and relatively low NO levels (indicative of the aged air mass), as shown in Fig. 4. Inspection of the time series day by day also reveals the frequent transport of photochemically aged air masses containing elevated concentrations of $O_3$ (over 100 ppbv), CO and $NO_2$* to the study site during the late evening (figures not shown). Similarly, the MOZAIC aircraft measurements have also found ~60 ppbv on average of $O_3$ at around 1500 *m* a.s.l. over Beijing at 5:00–6:00 LT in summer (i.e., May–July; Ding et al., 2008), which is comparable to what we observed at Mt. Tai. These results imply the existence of the $O_3$-laden air in the nocturnal residual layer over the North China Plain region. Moreover, Ding et al. (2008) also showed in their Figure 11 that the $O_3$ enhancement extended from the surface up to about 2 km, further evidence that during the daytime Mt. Tai should be within the boundary layer and is sampling at a vertical level where ozone enhancements are expected.

### 3.2. Impact of long-range transport

Long-range transport associated with synoptic weather and large-scale circulations is an important factor for the variation of $O_3$ in rural areas (Wang et al., 2009; Ding et al., 2013; Lin M. et al., 2014; Zhang et al., 2016). To elucidate the history of air masses sampled at Mt. Tai, we analyzed the summertime climatological air mass transport pattern during 2003-2015 with the aid of cluster analysis of back trajectories. The NCEP reanalysis data and GDAS archive data (http://ready.arl.noaa.gov/archives.php) were used to compute trajectories during 2003-2004 and 2005-2015. The detailed methodology has been documented by Wang et al. (2009) and Xue et al. (2011). Briefly, three-dimensional 72-hour back trajectories were computed four times a day (i.e., 2:00, 8:00, 14:00 and 20:00 LT) for June–August with the Hybrid Single-Particle Lagrangian Integrated Trajectory model (HYSPLIT, v4.9; Draxler et al. 2009), with an endpoint of 300 *m* above ground level exactly

over Mt. Tai. All the trajectories were then categorized into a small number of major groups with the HYSPLIT built-in cluster analysis approach. Total spatial variance (TSV) and the variance between each trajectory component were calculated to determine the optimum number of clusters (Draxler et al., 2009).

A total of five air mass types were extracted for the summer period, with four identified for June and July–August respectively. These air mass types are named according to the regions they traversed, and are described as follows: "Marine and East China" (M&EC) – air masses from the southeast passing over the ocean and polluted central eastern China; "Northeast China" (NEC) – air masses from the north passing over Northeast China; "Central China" (CC) – air masses from the south moving slowly over central China; "Southeast China" (SEC) – air masses from the south moving fast from southeast China; "Mongolia and North China" (M&NC) – air masses from the northwest passing over Mongolia and central northern China.

The above identified major types of air masses are presented in Fig. 5. In June, M&EC was most frequent (57%), followed by CC (26%), NEC (9%) and M&NC (8%; only identified in June). During the July–August period, the most frequent air mass type was still M&EC (36%), then CC (29%) and NEC (29%), with a minor fraction of SEC (6%; only identified in July–August). Overall, the transport patterns in June and July–August are quite similar, and it is evident that southerly and easterly air flows (e.g., M&EC and CC) dominated the air mass transport to Mt. Tai in summer. Such patterns are believed to be driven by the summer Asian monsoon (Ding et al., 2008).

The chemical signatures of the different air masses were also inspected and summarized in Table 3. The air masses of M&EC, CC and NEC, which passed over several polluted regions of eastern China, contained higher abundances of $O_3$ (with averages of 89–94 ppbv in June and 64–77 ppbv in July–August), CO and $NO_2$*. In comparison, the more aged air masses of M&NC and SEC showed relatively lower concentrations of $O_3$ (78±21 ppbv for M&NC in June and 58±17 ppbv for SEC in July–August) and its precursors (except for $NO_2$* in the SEC air mass). In view of the higher frequency and higher $O_3$ levels of the M&EC, CC and NEC air masses, it could be concluded that the regions with

the greatest influence on $O_3$ at Mt. Tai in summer are primarily located in the southern and eastern parts of central eastern China.

### 3.3. Observed Ozone Trend

Figure 6 presents the monthly average hourly $O_3$ and MDA8 $O_3$ mixing ratios in June and July–August whenever available from 2003–2015 at Mt. Tai. The least square linear regression analysis reveals the significant increase of surface $O_3$ at Mt. Tai since 2003. Monthly mean $O_3$ values based on hourly data increased at rates of 1.7±1.0 ppbv $yr^{-1}$ (±95% confidence intervals) in June and 2.1±0.9 ppbv $yr^{-1}$ in July–August, and the increases were statistically significant ($p < 0.01$). For the monthly means based on MDA8 $O_3$, the fewer available data points (as we only have monthly average data during 2004–2005 from Kanaya et al., 2013) likely reduced the significance of the trend in June, with a positive by statistically insignificant increase (rate = 1.4±1.9 ppbv $yr^{-1}$; $p = 0.12$). However the site had a significant positive trend in July–August (rate = 2.2±1.2 ppbv $yr^{-1}$; $p < 0.01$). Therefore we conclude that summertime surface $O_3$ levels at Mt. Tai have increased over the period 2003–2015.

Given the fact that Mt. Tai is above the PBL at night when there is no photochemistry, the ambient $O_3$ levels before dawn (e.g., 2:00–5:00 LT) are representative of the regional baseline $O_3$. The diurnal variation in Fig. 3 shows a slight but steady decrease in $O_3$ concentrations overnight, which should arise from dry deposition. It was assumed that dry deposition was essentially the same every year and did not affect the derived trends. Figure 7 shows the monthly averaged late-night $O_3$ mixing ratios in June and July–August available from 2003–2015 at Mt. Tai. Again, positive trends were found. The rate of increase was quantified at 1.9±1.8 ppbv $yr^{-1}$ ($p = 0.04$, significant) in June and 1.1±1.2 ppbv $yr^{-1}$ ($p = 0.06$, insignificant) during July–August. The increase of regional baseline likely explains the observed $O_3$ rise at Mt. Tai in June and also accounts for the majority of the increase during July–August. These results indicate the significant increase of surface $O_3$ in summer on the regional scale across northern China.

Table 4 compares the surface and lower tropospheric ozone trends available in East Asia in recent decades. Two aspects are particularly noteworthy from this comparison. First, most studies have

deduced significant positive trends demonstrating the broad increase of tropospheric $O_3$ over East Asia, especially in China. This pattern is distinct from that found in Europe and the eastern U.S., where $O_3$ levels have begun to decrease or level off since the 1990s or 2000s (e.g., Cooper et al., 2014; Lefohn et al., 2010; Oltmans et al., 2013; Parrish et al., 2012). The $O_3$ increase in East Asia is expected due to the rapid economic growth and increasing anthropogenic emissions of $O_3$ precursors in the past three decades (*e.g.,* Ohara et al., 2007). Second, the magnitude of $O_3$ increase is quite heterogeneous in different regions and the fastest rise was found in the North China Plain. For example, the rates of $O_3$ increase were in the range of 0.54-0.58 ppbv $yr^{-1}$ in Hong Kong (1994-2007, Wang et al., 2009; 2002-2013, Xue et al., 2014), 0.54 ppbv $yr^{-1}$ in Taiwan (1994-2007, Lin et al., 2010), 0.26-0.55 ppbv $yr^{-1}$ over South Korea (1990-2010, Lee et al., 2013; 1999-2010, Seo et al., 2014), 0.22-0.37 ppbv $yr^{-1}$ in major Japanese metropolitan areas (1990-2010; Akimoto et al., 2015), 0.64 ppbv $yr^{-1}$ at Mt. Happo, Japan (1991-2011, summer scenario; Parrish et al., 2014), and 0.15 ppbv $yr^{-1}$ at Mt. Waliguan, a GAW station in western China (1994-2013, summer scenario; Xu et al., 2016). According to the MOZAIC aircraft observations, in comparison, Ding et al. (2008) have reported the PBL $O_3$ increases of ~1 ppbv $yr^{-1}$ for the annual average and ~3 ppbv $yr^{-1}$ for the summer afternoon peaks over the period of 1995-2005. Zhang et al. (2014) analyzed their field measurements at an urban site in Beijing during 2005-2011 and quantified an increasing rate of 2.6 ppbv $yr^{-1}$ for the daytime average $O_3$ in summer. Comparable rates of $O_3$ increase (1.7-2.1 ppbv $yr^{-1}$) were determined in the present study from the measurements of longer time coverage and at a more regionally representative mountain site, affirming the significant rise of surface $O_3$ levels over the North China Plain region. Furthermore, the magnitude of $O_3$ increase in this region is also among the highest records currently reported in the world (Cooper et al., 2012 and 2014; Lin M. et al., 2014; Parrish et al., 2014).

### 3.4. Comparison with multi-decadal chemistry-climate simulations

We draw on a multi-decadal GFDL-AM3 chemical transport model simulation to provide context for the trends derived from the short observation record. In contrast to the free-running models used in Cooper *et al*. (2014) that generate their own metrology, the GFDL-AM3 simulations used in the present study are relaxed to the NCEP/NCAR reanalysis using a pressure-dependent nudging technique (Lin M.

et al., 2012) and thus allow for an apples-to-apples comparison with the observational records. The simulations are described in detail in a few recent publications, which show that AM3 captures inter-annual variability and long-term trends of baseline $O_3$ measured at Mauna Loa Observatory (Lin M. et al., 2014), western U.S. free tropospheric and surface sites (Lin M. et al., 2015a,b). Ozone measurements at Mt. Tai provide an important test for the model to represent $O_3$ trends in a polluted region where emissions have changed markedly over the past few decades.

Figure 8 shows comparisons of $O_3$ trends at Mt Tai as observed and simulated by the GFDL-AM3 model for June and July-August, respectively. The model has a mean state ozone bias of 10-20 ppbv as in the other global models (Fiore et al., 2009). For illustrative purposes, both observations and model results in Figure 8 are shown as anomalies. With anthropogenic emissions varying over time (based on Lamarque et al. (2010) with annual interpolation after 2000 to RCP 8.5), AM3 simulates significant MDA8 $O_3$ increases of $1.04 \pm 0.45$ ppbv $yr^{-1}$ over 1995-2014 for June and $1.65 \pm 0.41$ ppbv $yr^{-1}$ for July-August. A greater rate of $O_3$ increase is simulated for July-August with warmer temperatures compared to June, consistent with the trends derived from the shorter observational records. With constant emissions, AM3 gives no significant long-term ozone trends over the entire 1980-2014 period despite large inter-annual variability (see gray lines in Figure 8). The model indicates that changes in regional emissions have raised surface ozone over the North China Plain by ~30 ppbv in June and ~45 ppbv in July-August over the past 35 years, with an accelerating trend in the most recent 20 years.

### 3.5. Roles of meteorology and anthropogenic emissions

To further elucidate the factors contributing to the observed surface $O_3$ change at Mt. Tai, we examined variations in both meteorological conditions and anthropogenic emissions of $O_3$ precursors during the past decade. Table 2 shows year-to-year variability in summertime mean meteorological conditions including average temperature, RH, and prevailing wind direction recorded at Mt. Tai over the period of 2003–2015. No systematic change was found with regard to the overall meteorological conditions although some variability is clearly shown. For instance, substantially warmer temperatures were recorded in June 2015 and July-August 2013 as a result of large-scale heat waves (Yuan et al.,

2016). During these years, the GFDL-AM3 model with constant emissions simulates high-$O_3$ anomalies (up to ~10 ppbv) relative to the climatological mean (Figure 8), indicating that heat waves can enhance summertime $O_3$ pollution in Central Eastern China. Unfortunately, there were no observations available in 2005 and 2013. Observations show greater $O_3$ levels during July-August of 2014-2015 compared to 2004-2009 (Figure 8) but no significant change in temperature were found between the two time periods (Table 2), indicating the key role of regional emission changes in contributing to the observed ozone increase at Mt Tai.

We also explored the air mass transport pattern deduced from cluster analysis of back trajectories (see Section 3.2) year by year over 2003–2015 (*Table S1*). Despite the large year-to-year variability, again, no systematic change in the air mass transport pattern was indicated during the target period. Although the impact of meteorology on tropospheric $O_3$ is very complex and might not be quantified by such a simple analysis, the significant increase of surface $O_3$ observed at Mt. Tai should not primarily arise from the change in meteorological conditions.

We analyzed the satellite retrievals of formaldehyde (HCHO) and $NO_2$ to track the variations in the abundances of $O_3$ precursors (i.e., $NO_x$ and VOCs) during the study period. Considering that HCHO is a major oxidation product of a variety of VOC species and due to the availability of the satellite-retrieved products, HCHO was selected as an indicator of the VOC abundances. The satellite data were obtained from SCIAMACHY for 2003–2011 and GOME-2(B) from 2013 onwards, with the Level-2 products taken from the TEMIS archive (Tropospheric Emission Monitoring Internet Service; http://www.temis.nl/index.php). Considering the geographical representativeness of Mt. Tai, a larger domain (32 °–38 ° N, 115 °–120 ° E; see *Fig. 5*) was selected to process the regional mean satellite data. The monthly averaged HCHO and $NO_2$ column densities in June and July–August from 2003–2015 are documented in Fig. 9. Significant positive trends are seen for HCHO, with rates of 2.7%±2.2% ($p$ = 0.02) for June and 2.2%±1.4% ($p < 0.01$) for July–August, indicative of the strong increase of VOCs in this region. This result agrees very well with the emission inventory estimates which showed significant increases of anthropogenic VOC emissions in China in the past decades (Bo et al., 2008; Wang et al.,

2014), and is consistent with the lack of nationwide VOC controls. All of these results evidence the increase of atmospheric VOC abundances over the North China Plain.

What is more interesting is the two-phase variation of the $NO_2$ column, showing a significant increase first from 2003 to 2011 (June: 4.8%±3.4%, $p$ = 0.01; July–August: 7.7%±3.6%, $p$ < 0.01) and a decrease afterwards (see Fig. 9b). These satellite observations agree very well with the bottom-up emission inventory estimates, which clearly showed a break point occurring in 2011 in the anthropogenic $NO_x$ emissions of China (see *Fig. S2*). China has just launched a national $NO_x$ control programme during its "Twelfth Five-Year Plan" (i.e., 2011–2015) (China State Council, 2011). The strict control measures are very efficient and have resulted in an immediate reduction of $NO_x$ emissions, as affirmed by both emission inventories and satellite retrievals. Furthermore, the reduced levels of $NO_x$ in the most recent five years were also evidenced by our limited in-situ $NO_x$* measurements at Mt. Tai. As shown in Fig. 10, the ambient $NO_2$* levels in 2014 and 2015 were indeed substantially lower than those measured in the previous years before 2010.

From the above analyses, the $O_3$ increase between 2003 and 2011 is easy to understand in light of the consistent increase of both $NO_x$ and VOCs. For the later period, i.e. after 2011, in comparison, opposite trends have taken place with $NO_x$ decreasing but VOCs still increasing. The observed continuing $O_3$ rise suggests that the reduction of $NO_x$ is not adequate to reduce the ambient $O_3$ levels, with a background of increasing VOCs. We then evaluated the ozone production efficiency (OPE) for the air masses sampled at Mt. Tai. OPE is usually derived from the regression slope of the scatter plots of $O_3$ versus $NO_z$ (Trainer et al., 1993), and is a useful metric to infer how efficient $O_3$ is produced per oxidation of unit of $NO_x$ (e.g., Wang et al., 2010; Xue et al., 2011). As $NO_y$ (and thus $NO_z$) is not routinely measured in the present study, $NO_2$* is used instead of $NO_z$ to infer the OPE values. It should be reasonable considering that our measured $NO_2$* significantly overestimated true $NO_2$ and actually contained a large fraction of $NO_z$, especially in the afternoon period when $NO_z$ was at its maximum with $NO_2$ at the minimum (Xu et al., 2013). The scatter plots of $O_3$ versus $NO_2$* during the afternoon hours (i.e., 12:00–18:00 LT) available from 2006–2015 at Mt. Tai are presented in Fig. 11. The OPE

values in 2014–2015 (i.e., 9.6-15.0) were significantly higher than those determined during 2006–2009 (i.e., 3.6-7.9). This demonstrates the greater ozone production efficiency in recent years with increasing VOCs. These results indicate that although $NO_x$ in China has been reduced since 2011, little action on VOC control has led to increased emissions of VOCs, which could make $O_3$ formation more efficient per unit of $NO_x$. As a consequence, ambient $O_3$ levels have been rising in northern China. We conclude that control of VOCs is urgently needed, in addition to the ongoing strict $NO_x$ control, to mitigate regional $O_3$ pollution in China.

## 4. Conclusions

We have compiled all field observations of $O_3$ and its precursors ever collected at Mt. Tai in the North China Plain and found a significant increase of summertime surface $O_3$ over 2003–2015 at this regionally representative site. The ozone increase derived from these valuable but sparse observations is supported by a chemistry-climate model simulation with emissions varying from 1980 to 2014. The marked increase of surface $O_3$ levels over central Eastern China is primarily attributable to rising anthropogenic emissions of $O_3$ precursors. We provide evidence that the changes in VOCs emissions contribute to the observed ozone increase since 2011 when $NO_x$ has reduced efficiently as a result of a strict national emission control programme. This study provides some evidence that the current Chinese control programme, focusing on $NO_x$ alone with little action for VOCs, is not sufficient for mitigating regional $O_3$ pollution, and calls on the implementation of VOC controls as soon as possible. Similar to the U.S., China phased in its air pollution control measures resulting in decreasing $SO_2$ emission after 2006 and $NO_x$ emission after 2011. It is foreseen that the national VOC control will be launched very soon. Thus, follow-up long-term measurements are required to evaluate the response of ambient $O_3$ to the upcoming VOC control and to provide observational constraints to evaluate global and regional chemical transport models.

## Acknowledgements

The authors thank Steven Poon and Wei Nie for their contributions to the field study, and the staff of the Mt. Tai Meteorological Observatory for the logistics and help during the field measurements. We

are also grateful to the NOAA Air Resources Laboratory for providing the HYSPLIT model and meteorological data, and the European Space Agency for the free distribution of SCIAMACHY and GOME-2(B) satellite data through the TEMIS website (http://www.temis.nl/index.php). This work was supported by the National Natural Science Foundation of China (project no.: 41275123) and the Qilu Youth Talent Programme of Shandong University.

**References**

Akimoto, H., Mori, Y., Sasaki, K., Nakanishi, H., Ohizumi, T., and Itano, Y.: Analysis of monitoring data of ground-level ozone in Japan for long-term trend during 1990-2010: Causes of temporal and spatial variation, *Atmos. Environ.*, 102, 302-310, 2015.

Bo, Y., Cai, H., and Xie, S. D.: Spatial and temporal variation of historical anthropogenic NMVOCs emission inventories in China, *Atmos. Chem. Phys.*, 8, 7297-7316, 2008.

China State Council: Twelfth Five-Year Plan on National Economy and Social Development of the People's Republic of China, 2011. http://www.gov.cn/2011lh/content_1825838.htm (in Chinese).

Cooper, O. R., Gao, R.-S., Tarasick, D., Leblanc, T., and Sweeney, C.: Long-term ozone trends at rural ozone monitoring sites across the United States, 1990–2010, *J. Geophys. Res. –Atmos.*, 117, D22307, doi: 10.1029/2012jd018261, 2012.

Cooper, O. R., Parrish, D. D., Ziemke, J., Balashov, N. V., Cupeiro, M., Galbally, I. E., Gilge, S., Horowitz, L., Jensen, N. R., Naik, V., Oltmans, S. J., Schwab, J., Shindell, D. T., Thompson, A. M., Thouret, V., Wang, Y., and Zbinden, R. M.: Global distribution and trends of tropospheric ozone: An observation-based review, *Elementa Sci. of Anth.*, 2, 000029, 2014.

Crutzen, P.: A discussion ofthe chemistry of some minor constituents in the stratosphere and troposphere, *Pure Appl. Geophys.*, 106-108, 1385-1399, 1973.

Ding, A. J., Wang, T., Thouret, V., Cammas, J.-P., and Nédélec, P.: Tropospheric ozone climatology over Beijing: analysis of aircraft data from the MOZAIC program, *Atmos. Chem. Phys.*, 8, 1-13, 2008.

Ding, A. J., Fu, C. B., Yang, X. Q., Sun, J. N., Zheng, L. F., Xie, Y. N., Herrmann, E., Nie, W., Petaja, T., Kerminen, V.-M., and Kulmala, M.: Ozone and fine particle in the western Yangtze River Delta: an overview of 1 yr data at the SORPES station, *Atmos. Chem. Phys.*, 13, 5813-5830, 2013.

Draxler, R. R., Stunder, B., Rolph, G., and Taylor, A.: HYSPLIT4 user's guide, http://ready.arl.noaa.gov/HYSPLIT_info.php, 2009.

Fine, R., Miller, M. B., Burley, J., Jaffe, D. A., Pierce, R. B., Lin, M., and Gustin, M. S.: Variability and sources of surface ozone at rural sites in Nevada, USA: Results from two years of the Nevada Rural Ozone Initiative, *Sci. Total Environ.*, 530–531, 471-482, 2015.

Fiore, A. M., Dentener, F. J., Wild, O., Cuvelier, C., Schultz, M. G., Hess, P., Textor, C., Schulz, M., Doherty, R. M., Horowitz, L. W., MacKenzie, I. A., Sanderson, M. G., Shindell, D. T., Stevenson, D. S., Szopa, S., van Dingenen, R., Zeng, G., Atherton, C. S., Bergmann, D. J., Bey, I., Carmichael, G. R., Collins, W. J., Duncan, B. N., Faluvegi, G., Folberth, G. A., Gauss, M., Gong, S., Hauglustaine, D., Holloway, T., Isaksen, I. S. A., Jacob, D. J., Jonson, J. E., Kaminski, J. W., Keating, T. J., Lupu, A., Marmer, E., Montanaro, V., Park, R. J., Pitari, G., Pringle, K. J., Pyle, J. A., Schroeder, S., Vivanco, M. G., Wind, P., Wojcik, G., Wu, S., and Zuber, A.: Multimodel estimates of intercontinental source receptor relationships for ozone pollution, *J. Geophys. Res.-Atmos.*, 114, D04301, doi:10.1029/2008JD010816, 2009.

Gao, J., Wang, T., Ding, A. J., and Liu, C. B.: Observational study of ozone and carbon monoxide at the summit of mount Tai (1534m asl) in central-eastern China, *Atmos. Environ.*, 39, 4779-4791, 2005.

Guo, J., Wang, Y., Shen, X., Wang, Z., Lee, T., Wang, X., Li, P., Sun, M., Collett Jr, J. L., Wang, W., and Wang, T.: Characterization of cloud water chemistry at Mount Tai, China: Seasonal variation, anthropogenic impact, and cloud processing, *Atmos. Environ.*, 60, 467-476, 2012.

IPCC: Climate Change: The Assessment Reports of the Intergovernmental Pane on Climate Change, Cambridge University Press, Cambridge, UK, 2013.

Kanaya, Y., Akimoto, H., Wang, Z. F., Pochanart, P., Kawamura, K., Liu, Y., Li, J., Komazaki, Y., Irie, H., and Pan, X. L., Taketani, F., Yamaji, K., Tanimoto, H., Inomata, S., Kato, S., Suthawaree, J., Okuzawa, K., Wang, G., Aggarwal, S. G., Fu, P. Q., Wang, T., Gao, J., Wang, Y., and Zhuang, G. S.: Overview of the Mount Tai Experiment (MTX2006) in central East China in June 2006: studies of significant regional air pollution, *Atmos. Chem. Phys.*, 13, 8265-8283, 2013.

Lamarque, J.-F., Bond, T. C., Eyring, V., Granier, C., Heil, A., Klimont, Z., Lee, D., Liousse, C., Mieville, A., Owen, B., Schultz, M. G., Shindell, D., Smith, S. J., Stehfest, E., van Aardenne, J., Cooper, O. R., Kainuma, M., Mahowald, N., Mc-Connell, J. R., Naik, V., Riahi, K., and van Vuuren, D. P.: Historical (1850-2000) gridded anthropogenic and biomass burning emissions of reactive gases and aerosols: methodology and application, *Atmos. Chem. Phys.*, 10, 7017–7039, 2010.

Lee, H.-J., Kim, S.-W., Brioude, J., Cooper, O. R., Frost, G. J., Kim, C.-H., Park, R. J., Trainer, M., and Woo, J.-H.: Transport of $NO_x$ in East Asia identified by satellite and in situ measurements and Lagrangian particle dispersion model simulations, *J. Geophys. Res. Atmos.*, 119, 2574-2596, 2013.

Lefohn, A. S., Shadwick, D., and Oltmans, S. J.: Characterizing changes in surface ozone levels in metropolitan and rural areas in the United States for 1980–2008 and 1994–2008, *Atmos. Environ.*, 44, 5199-5210, 2010.

Lin, M., Holloway, T., Oki, T., Streets, D. G., and Richter, A.: Multi-scale model analysis of boundary layer ozone over East Asia, *Atmos. Chem. Phys.*, 9, 3277-3301, 2009.

Lin, M., Fiore, A. M., Horowitz, L. W., Cooper, O. R., Naik, V., Holloway, J., Johnson, B. J., Middlebrook, A. M., Oltmans, S. J., Pollack, I. B., Ryerson, T. B., Warner, J. X., Wiedeninmyer, C., Wilson, J., and Wyman, B.: Transport of Asian ozone pollution into surface air over the western United States in spring, *J. Geophys. Res.-Atmos.*, 117, D00V07, doi:10.1029/2011JD016961, 2012.

Lin, M., Horowitz, L. W., Oltmans, S. J., Fiore, A. M., and Fan, S.: Tropospheric ozone trends at Mauna Loa Observatory tied to decadal climate variability, *Nature Geosci.*, 7, 136-143, 2014.

Lin, M., Fiore, A. M., Horowitz, L. W., Langford, A. O., Oltmans, S. J., Tarasick, D., and Rieder, H. E.: Climate variability modulates western US ozone air quality in spring via deep stratospheric intrusions, *Nat. Commun.*, 6, 7105, 2015a.

Lin, M., Horowitz, L. W., Cooper, O. R., Tarasick, D., Conley, S., Iraci, L. T., Johnson, B., Leblanc, T., Petropavlovskikh, I., and Yates, E. L.: Revisiting the evidence of increasing springtime ozone mixing ratios in the free troposphere over western North America, *Geophys. Res. Lett.*, 42, 8719–8728, 2015b.

Lin, W., Xu, X., Zhang, X., and Tang, J.: Contributions of pollutants from North China Plain to surface ozone at the Shangdianzi GAW Station, *Atmos. Chem. Phys.*, 8, 5889-5898, 2008.

Lin, Y.-K., Lin, T.-H., and Chang, S.-C.: The changes in different ozone metrics and their implications following precursor reductions over northern Taiwan from 1994 to 2007, *Environ. Monit. Assess.*, 169, 143-157, 2010.

Logan, J. A., Staehelin, J., Megretskaia, I. A., Cammas, J.-P., Thouret, V., Claude, H., De Backer, H., Steinbacher, M., Scheel, H.-E., Stübi, R., Fröhlich, M., and Derwent, R.: Changes in ozone over Europe: Analysis of ozone measurements from sondes, regular aircraft (MOZAIC) and alpine surface sites, *J. Geophys. Res.-Atmos.*, 117, D09301, doi: 10.1029/2011jd016952, 2012.

Lu, Z., Streets, D. G., Zhang, Q., Wang, S., Carmichael, G. R., Cheng, Y. F., Wei, C., Chin, M., Diehl, T., and Tan, Q.: Sulfur dioxide emissions in China and sulfur trends in East Asia since 2000, *Atmos. Chem. Phys.*, 10, 6311-6331, 2010.

Ma, J., Zhou, X., and Hauglustaine, D.: Summertime tropospheric ozone over China simulated with a regional chemical transport model 2. Source contributions and budget, *J. Geophys. Res.-Atmos.*, 107 (D22), 4612, doi:10.1029/2001jd001355, 2002.

Monks, P. S., Archibald, A., Colette, A., Cooper, O., Coyle, M., Derwent, R., Fowler, D., Granier, C., Law, K. S., Mills, G. E., Stevenson, D. S., Tarasova, O., Thouret, V., von Schneidemesser, E., Sommariva, R., Wild, O., and Williams, M. L.: Tropospheric ozone and its precursors from the urban to the global scale from air quality to short-lived climate forcer, *Atmos. Chem. Phys.*, 15, 8889-8973, 2015.

National Research Council: Rethinking the Ozone Problem in Urban and Regional Air Pollution, *Natl. Acad. Press*, Washington, D. C., 1991.

Ohara, T., Akimoto, H., Kurokawa, J.-I., Horii, N., Yamaji, K., Yan, X., and Hayasaka, T.: An Asian emission inventory of anthropogenic emission sources for the period 1980–2020, *Atmos. Chem. Phys.*, 7, 4419-4444, 2007.

Oltmans, S. J., Lefohn, A. S., Shadwick, D., Harris, J. M., Scheel, H. E., Galbally, I., Tarasick, D. W., Johnson, B. J., Brunke, E.-G., Claude, H., Zeng, G., Nichol, S., Schmidlin, F., Davies, J., Cuevas, E., Redondas, A., Naoe, H., Nakano, T., and Kawasato, T.: Recent tropospheric ozone changes - A pattern dominated by slow or no growth, *Atmos. Environ.*, 67, 331-351, 2013.

Parrish, D. D., Law, K. S., Staehelin, J., Derwent, R., Cooper, O. R., Tanimoto, H., Volz-Thomas, A., Gilge, S., Scheel, H. E., Steinbacher, M., and Chan, E.: Long-term changes in lower tropospheric baseline ozone concentrations at northern mid-latitudes, *Atmos. Chem. Phys.*, 12, 11485-11504, 2012.

Parrish, D. D., Lamarque, J. F., Naik, V., Horowitz, L., Shindell, D. T., Staehelin, J., Derwent, R., Cooper, O., Tanimoto, H., Volz-Thomas, A., Gilge, S., Scheel, H.-E., Steinbacher, M., and Chan, E.: Long-term changes in lower tropospheric baseline ozone concentrations: Comparing chemistry-climate models and observations at northern midlatitudes, *J. Geophys. Res.-Atmos.*, 119, 5719-5736, doi:10.1002/2013jd021435, 2014.

Seinfeld, J. H., and Pandis, S. N.: Atmospheric Chemistry and Physics: From Air Pollution to Climate Change., Wiley, 2006.

Seo, J., Youn, D., Kim, J., and Lee, H.: Extensive spatiotemporal analyses of surface ozone and related meteorological variables in South Korea for the period 1999–2010, *Atmos. Chem. Phys.*, 14, 6395-6415, 2014.

Shen, X., Lee, T., Guo, J., Wang, X., Li, P., Xu, P., Wang, Y., Ren, Y., Wang, W., Wang, T., Li, Y., Carn, S. A., and Collett Jr, J. L.: Aqueous phase sulfate production in clouds in eastern China, *Atmos. Environ.*, 62, 502-511, 2012.

Shindell, D., Kuylenstierna, J. C., Vignati, E., van Dingenen, R., Amann, M., Klimont, Z., Anenberg, S. C., Muller, N., Janssens-Maenhout, G., Raes, F., Schwartz, J., Faluvegi, G., Pozzoli, L., Kupianinen, K., H-Isaksson, L., Emberson, L., Streets, D., Ramanathan, V., Hicks, K., Oanh, N. T., Milly, G.,

Williams, M., Demkine, V., and Fowler, D.: Simultaneously mitigating near-term climate change and improving human health and food security, *Science*, 335, 183-189, 2012.

Stevenson, D. S., Young, P. J., Naik, V., Lamarque, J.-F., Shindell, D. T., Voulgarakis, A., Skeie, R., Dalsoren, S. B., Myhre, G., Berntsen, T. K., Folberth, G. A., Rumbold, S. T., Collins, W. J., Mackenzie, I. A., Doherty, R. M., Zeng, G., van Noijie, T. P. C., Strunk, A., Bergmann, D., Cameron-Smith, P., Plummer, D. A., Strode, S. A., Horowitz, L., Lee, Y. H., Szopa, S., Sudo, K., Nagashima, T., Josse, B., Cionni, I., Righi, M., Eyring, V., Conley, A., Bowman, K. W., Wild, O., and Archibald, A.: Tropospheric ozone changes, radiative forcing and attribution to emissions in the Atmospheric Chemistry and Climate Model Intercomparison Project (ACCMIP), *Atmos. Chem. Phys.*, 13, 3063-3085, 2013.

Stohl, A., Bonasoni, P., Cristofanelli, P., Collins, W. J., Feichter, J., Frank, A., Forster, C., Gerasopoulos, E., Gäggeler, H., James, P., Kentarchos, T., Kromp-Kalb, H., Kruger, B., Land, C., Meloen, J., Papayannis, A., Priller, A., Seibert, P., Sprenger, M., Roelofs, G. J., Scheel, H. E., Schnabel, C., Siegmund, P., Tobler, L., Trickl, T., Wernli, H., Wirth, V., Zanis, P., and Zerefos, C.: Stratosphere-troposphere exchange: A review, and what we have learned from STACCATO, *J. Geophys. Res.-Atmos.*, 108, 8516, doi:10.1029/2002jd002490, 2003.

Suthawaree, J., Kato, S., Okuzawa, K., Kanaya, Y., Pochanart, P., Akimoto, H., Wang, Z., and Kajii, Y.: Measurements of volatile organic compounds in the middle of Central East China during Mount Tai Experiment 2006 (MTX2006): observation of regional background and impact of biomass burning, *Atmos. Chem. Phys.*, 10, 1269-1285, 2010.

Tang, G., Li, X., Wang, Y., Xin, J., and Ren, X.: Surface ozone trend details and interpretations in Beijing, 2001–2006, *Atmos. Chem. Phys.*, 9, 8813-8823, 2009.

The Royal Society: Ground-level Ozone in the 21st century: Future Trends, Impacts and Policy Implications, Royal Society policy document 15/08, RS1276, 2008. Available at http://royalsociety.org/Report_WF.aspx?pageid57924&terms5groundlevel1ozone.

Trainer, M., Parrish, D. D., Buhr, M. P., Norton, R. B., Fehsenfeld, F. C., Anlauf, K. G., Bottenheim, J. W., Tang, Y. Z., Wiebe, H. A., Roberts, J. M., Tanner, R. L., Newman, L., Bowersox, V. C., Meagher, J. F., Olszyna, K. J., Rodgers, M. O., Wang, T., Berresheim, H., Demerjian, K. L., Roychowdhury, U. K.: Correlation of ozone with $NO_y$ in photochemically aged air, *J. Geophys. Res.-Atmos.*, 98 (D2), 2917-2925, doi:10.1029/92jd01910, 1993.

UNEP and WMO: Integrated Assessment of black carbon and tropospheric ozone: Summary for decision makers, United Nations Environment Programme, Nairobi, Kenya, 2011.

Wang, S. X., Zhao, B., Cai, S., Klimont, Z., Nielsen, C. P., Morikawa, T., Woo, J. H., Kim, Y., Fu, X., Xu, J. Y., Hao, J. M., and He, K. B.: Emission trends and mitigation options for air pollutants in East Asia, *Atmos. Chem. Phys.*, 14, 6571-6603, 2014.

Wang, T., Wei, X. L., Ding, A. J., Poon, C. N., Lam, K. S. , Li, Y. S., Chan, L. Y., and Anson, M.: Increasing surface ozone concentrations in the background atmosphere of Southern China, 1994–2007, *Atmos. Chem. Phys.*, 9, 6217-6227, 2009.

Wang, T., Nie, W., Gao, J., Xue, L. K., Gao, X. M., Wang, X. F., Qiu, J., Poon, C. N., Meinardi, S., Blake, D. R., Wang, S. L., Ding, A. J., Chai, F. H., Zhang. Q. Z., and Wang. W. X.: Air quality during the 2008 Beijing Olympics: secondary pollutants and regional impact, *Atmos. Chem. Phys.*, 10, 7603-7615, 2010.

Warneke, C., de Gouw, J., Holloway, J., Peischl, J., Ryerson, T., Atlas, E., Blake, D., Trainer, M., and Parrish, D.: Multiyear trends in volatile organic compounds in Los Angeles, California: five decades of decreasing emissions, *J. Geophys. Res.-Atmos.*, 117, D00V17, doi:10.1029/2012JD017899, 2012.

Xu, W., Lin, W., Xu, X., Tang, J., Huang, J., Wu, H., and Zhang, X.: Long-term trends of surface ozone and its influencing factors at the Mt Waliguan GAW station, China–Part 1: Overall trends and characteristics, *Atmos. Chem. Phys.*, 16, 6191-6205, 2016.

Xu, X., Lin, W., Wang, T., Yan, P., Tang, J., Meng, Z., and Wang, Y.: Long-term trend of surface ozone at a regional background station in eastern China 1991–2006: enhanced variability, *Atmos. Chem. Phys.*, 8, 2595-2607, 2008.

Xu, Z., Wang, T., Xue, L. K., Louie, P. K. K., Luk, C. W. Y., Gao, J., Wang, S. L., Chai, F. H., and Wang, W. X.: Evaluating the uncertainties of thermal catalytic conversion in measuring atmospheric nitrogen dioxide at four differently polluted sites in China, *Atmos. Environ.*, 76, 221-226, 2013.

Xue, L. K., Wang, T., Zhang, J. M., Zhang, X. C., Deligeer, Poon, C. N., Ding, A. J., Zhou, X. H., Wu, W. S., Tang, J., Zhang, Q. Z., and Wang, W. X.: Source of surface ozone and reactive nitrogen speciation at Mount Waliguan in western China: New insights from the 2006 summer study, *J. Geophys. Res.-Atmos.*, 116 (D7), D07306, doi:10.1029/2010jd014735, 2011.

Xue, L. K., Wang, T., Louie, P. K. K., Luk, C. W. Y., Blake, D. R., and Xu, Z.: Increasing external effects negate local efforts to control ozone air pollution: a case study of Hong Kong and implications for other Chinese cities, *Environ. Sci. Tech.*, 48, 10769-10775, 2014.

Yamaji, K., Ohara, T., Uno, I., Tanimoto, H., Kurokawa, J., and Akimoto, H.: Analysis of the seasonal variation of ozone in the boundary layer in East Asia using the Community Multiscale Air Quality model: What controls surface ozone levels over Japan?, *Atmos. Environ.*, 40, 1856–1868, 2006.

Yamaji, K., Li, J., Uno, I., Kanaya, Y., Irie, H., Takigawa, M., Komazaki, Y., Pochanart, P., Liu, Y., Tanimoto, H., Ohara, T., Yan, X., Wang, Z., and Akimoto, H.: Impact of open crop residual burning on air quality over Central Eastern China during the Mount Tai Experiment 2006 (MTX2006), *Atmos. Chem. Phys.*, 10, 7353-7368, 2010.

Yuan, W., Cai, W., Chen, Y., Liu, S., Dong, W., Zhang, H., Yu, G., Chen, Z., He, H., Guo, W., Liu, D., Liu S., Xiang, W., Xie, Z., Zhao, Z., and Zhou, G.: Severe summer heatwave and drought strongly reduced carbon uptake in Southern China, *Sci. Rep.*, 6, 18813, 2016.

Zhang, Q., Yuan, B., Shao, M., Wang, X., Lu, S., Lu, K., Wang, M., Chen, L., Chang, C.-C., and Liu, S.: Variations of ground-level $O_3$ and its precursors in Beijing in summertime between 2005 and 2011, *Atmos. Chem. Phys.*, 14, 6089-6101, 2014.

Zhang, Y., Ding, A., Mao, H., Nie, W., Zhou, D., Liu, L., Huang, X., Fu, C.: Impact of synoptic weather patterns and inter-decadal climate variability on air quality in the North China Plain during 1980-2013, *Atmos. Envion.*, 124, 119-128, 2016.

**Table 1.** The observations at Mt. Tai analyzed in the present study.

| Year | Month | Observed species | Data source |
|---|---|---|---|
| 2003 | Jul.-Nov. | $O_3$, CO | Gao et al. (2005) and our study |
| 2004 | Jun.-Aug. | $O_3$ | Kanaya et al.( 2013)[a] |
| 2005 | Jun.-Aug. | $O_3$ | Kanaya et al.( 2013)[a] |
| 2006 | Jun.-Dec. | $O_3$, $NO_2$*, NO | Our study |
| 2007 | Mar.-Dec. | $O_3$, NO, $NO_2$*, CO | Our study [b] |
| 2008 | Jan.-Dec. | $O_3$, NO, $NO_2$*, CO | Our study |
| 2009 | Jan.-Jun. | $O_3$, NO, $NO_2$*, CO | Our study |
| 2014 | Jun.-Aug. | $O_3$, NOx*, CO | Our study [c] |
| 2015 | Jun.-Aug. | $O_3$, NO, $NO_2$*, CO | Our study [c] |

[a] Monthly average data were taken from Kanaya et al. (2013).

[b] Valid NO and $NO_2$* data were only available in March-April and July-December, and CO was available in March-April in 2007.

[c] Note that the intensive measurement periods were 6 June – 3 July & 24 July – 26 August in 2014 and 14 June – 8 August in 2015.

**Table 2.** Summary of meteorological conditions recorded at Mt. Tai in June and July-August over 2003-2015[a].

| Year | June | | | July-August | | |
|---|---|---|---|---|---|---|
| | Temperature (℃) | RH (%) | Prevailing WD | Temperature (℃) | RH (%) | Prevailing WD |
| 2003 | 15.4±3.1 | 70.9±19.2 | SW | 17.3±2.9 | 88.3±16.3 | SW |
| 2004 | 15.4±3.9 | 74.4±21.2 | SW | 17.0±2.5 | 86.8±15.5 | SSW |
| 2005 | 18.1±3.2 | 65.0±22.0 | SSW | 17.4±2.9 | 86.8±16.3 | SW |
| 2006 | 17.2±2.9 | 67.8±21.4 | SSW | 18.3±2.0 | 88.3±16.3 | SSW |
| 2007 | 17.0±2.8 | 71.4±27.3 | E | 17.8±2.3 | 85.2±21.1 | E |
| 2008 | 15.0±3.6 | 76.9±20.0 | S | 17.0±2.3 | 86.3±14.6 | S |
| 2009 | 17.9±3.1 | 57.8±22.2 | SSW | 17.4±2.9 | 78.7±21.8 | S |
| 2010 | 15.9±3.6 | 80.1±18.7 | SW | 18.2±2.7 | 91.0±16.9 | SW |
| 2011 | 16.6±2.7 | 72.6±21.1 | SSW | 17.6±2.5 | 87.6±16.1 | S |
| 2012 | 16.8±3.2 | 71.0±23.8 | SW | 18.2±2.4 | 89.5±17.9 | E |
| 2013 | 16.1±3.1 | 79.8±19.6 | SW | 19.3±2.4 | 88.2±15.6 | SW |
| 2014 | 15.3±2.9 | 79.9±17.6 | SW | 16.5±2.3 | 86.7±14.6 | SW |
| 2015 | 15.8±2.8 | 70.5±21.0 | SW | 18.0±2.1 | 86.1±16.9 | SW |

[a] Average and standard deviations are provided.

**Table 3.** Statistics of $O_3$, $NO_2$* and CO in different air mass categories [a]

| June | | | | July-August | | | |
|---|---|---|---|---|---|---|---|
| Air mass [b] | $O_3$ | $NO_2$* | CO | Air mass [b] | $O_3$ | $NO_2$* | CO |
| M&EC | 92±27 | 7.2±5.3 | 500±300 | M&EC | 64±22 | 3.6±2.9 | 370±180 |
| CC | 89±24 | 6.3±5.0 | 550±300 | CC | 77±21 | 3.3±2.5 | 440±180 |
| NEC | 94±25 | 7.0±4.5 | 380±180 | NEC | 73±22 | 4.5±4.2 | 380±180 |
| M&NC | 78±21 | 4.0±3.3 | 280±180 | SEC | 58±17 | 4.1±2.4 | 350±80 |

[a] The unit is ppbv; average and standard deviations are provided.

[b] Refer to *Figure* 5 and Section 3.2 for the derivation and description of the air mass types.

**Table 4.** Summary of surface and lower tropospheric ozone trends recorded in East Asia.

| Station | Site type | Period | Rate of change (ppbv $yr^{-1}$) | Reference |
|---|---|---|---|---|
| Mt. Tai | rural | 2003-2015 (summer) | 1.7±1.0 (June)<br>2.1±0.9 (July-August) | This study |
| Beijing | rural (MOZAIC) | 1995-2005 | ~1 (annual average)<br>~3 (summer afternoon) | Ding et al. (2008) |
| Hong Kong (Hok Tsui) | rural | 1994-2007 | 0.58 | Wang et al. (2009) |
| Hong Kong | urban & suburban | 2002-2013 (autumn) | 0.54±0.49 | Xue et al. (2014) |
| Lin'an | rural | 1991-2006 | 2.7% (summer daily maximum) | Xu et al. (2008) |
| Waliguan | remote | 1994-2013 (summer) | 0.15±0.19 | Xu et al. (2016) |
| Taiwan (Yangming) | rural | 1994-2007 | 0.54±0.21 | Lin et al. (2010) |
| Mt. Happo, Japan | rural | 1991-2011 (summer) | 0.64±0.40 | Parrish et al. (2012) |
| Tokyo, Japan | urban & suburban | 1990-2010 | 0.31±0.02 | Akimoto et al. (2015) |
| Nagoya, Japan | urban & suburban | 1990-2010 | 0.22±0.05 | Akimoto et al. (2015) |
| Osaka/Kyoto, Japan | urban & suburban | 1990-2010 | 0.37±0.03 | Akimoto et al. (2015) |
| Fukuoka, Japan | urban & suburban | 1990-2010 | 0.37±0.04 | Akimoto et al. (2015) |
| South Korea | 124 urban sites average | 1999-2010 | 0.26 | Seo et al. (2014) |
| South Korea | 56 urban sites average | 1990-2010 | 0.48±0.07 (annual average)<br>0.55±0.13 (summer) | Lee et al. (2013) |

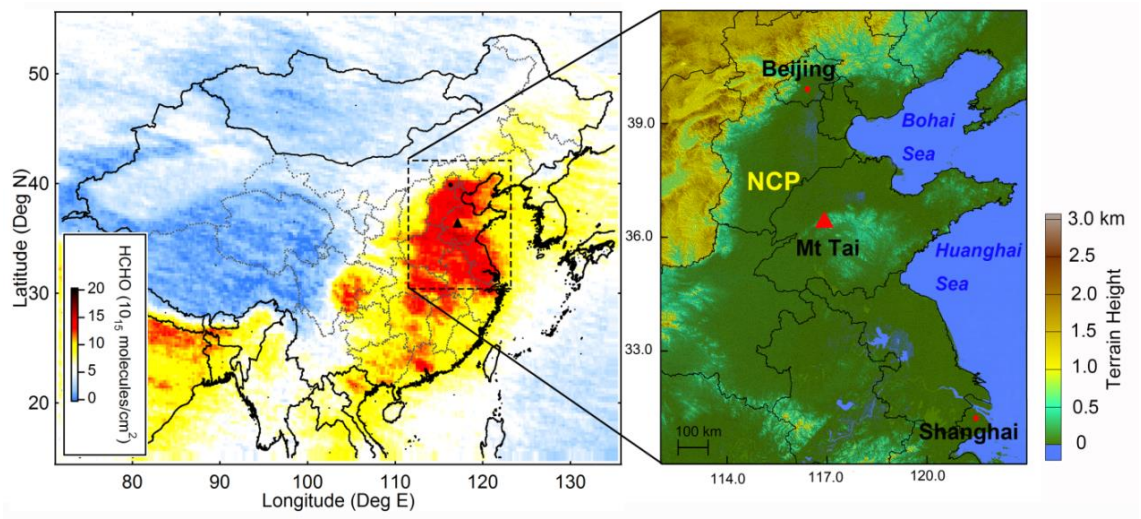


**Figure 1.** Geographical map showing the North China Plain and the location of Mt. Tai. The left map is color-coded by the HCHO column density in the summer period (JJA; 2003–2014) retrieved from SCIAMACHY and GOME-2(B).

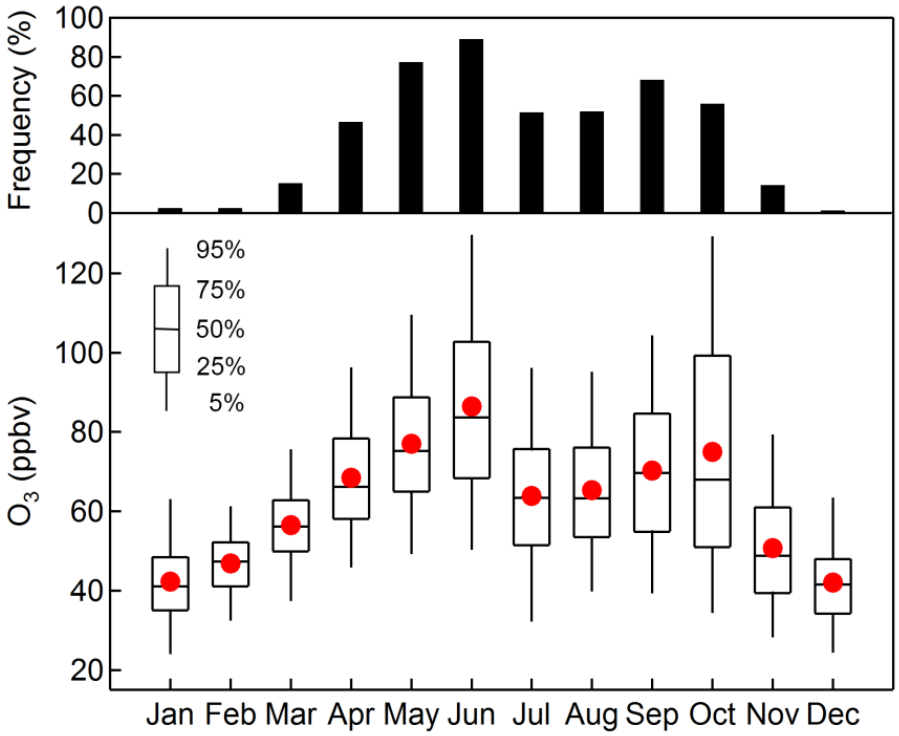


**Figure 2.** Seasonal variation of surface $O_3$ mixing ratios at Mt. Tai derived from the continuous observations from 2006–2009. Red dots indicate the monthly average $O_3$ concentrations. Shown in the upper panel is the frequency of the MDA8 $O_3$ exceeding the Chinese national ambient air quality standard, i.e. 75 ppbv (Class II).

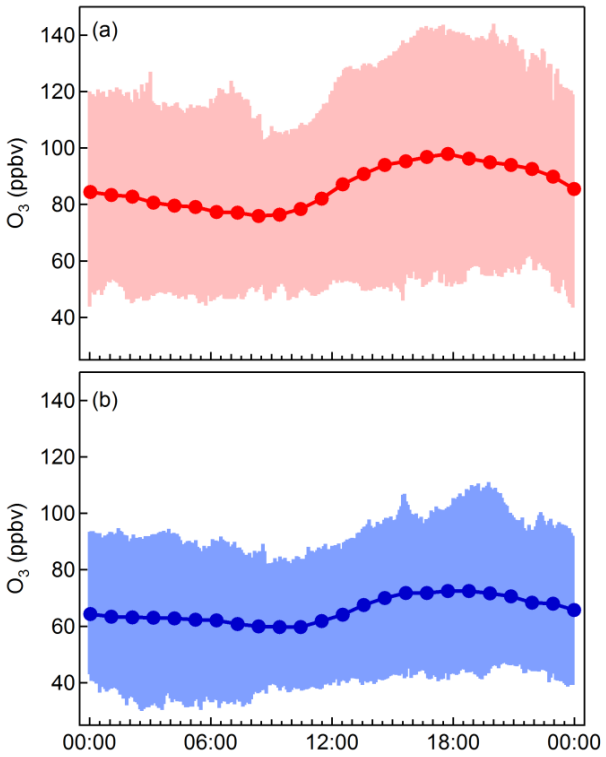


**Figure 3.** Average diurnal variations of surface $O_3$ at Mt. Tai in (a) June and (b) July-August derived from the continuous observations from 2006–2009. The shaded area indicates the 5$^{th}$ and 95$^{th}$ percentiles of the data.

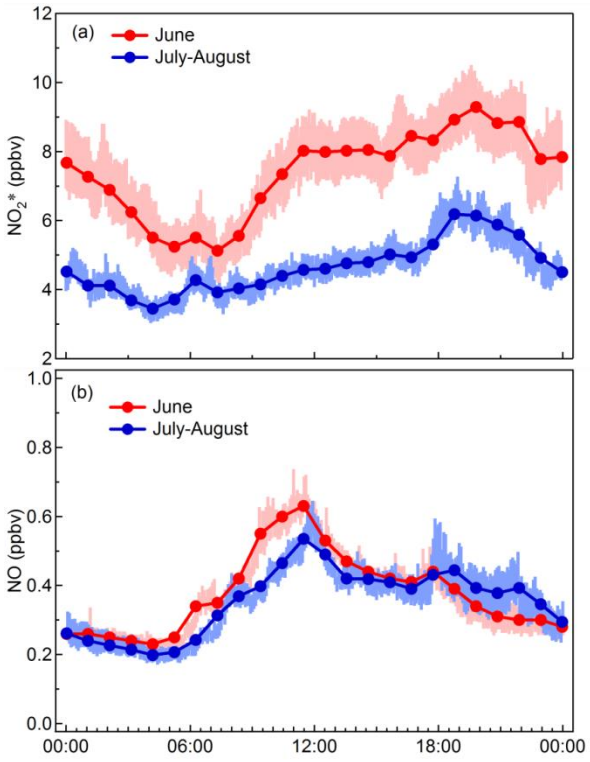


**Figure 4.** Average diurnal variations of (a) $NO_2$* and (b) NO at Mt. Tai in June and July-August derived from the continuous observations from 2006–2009. The shaded area indicates the standard error of the mean.

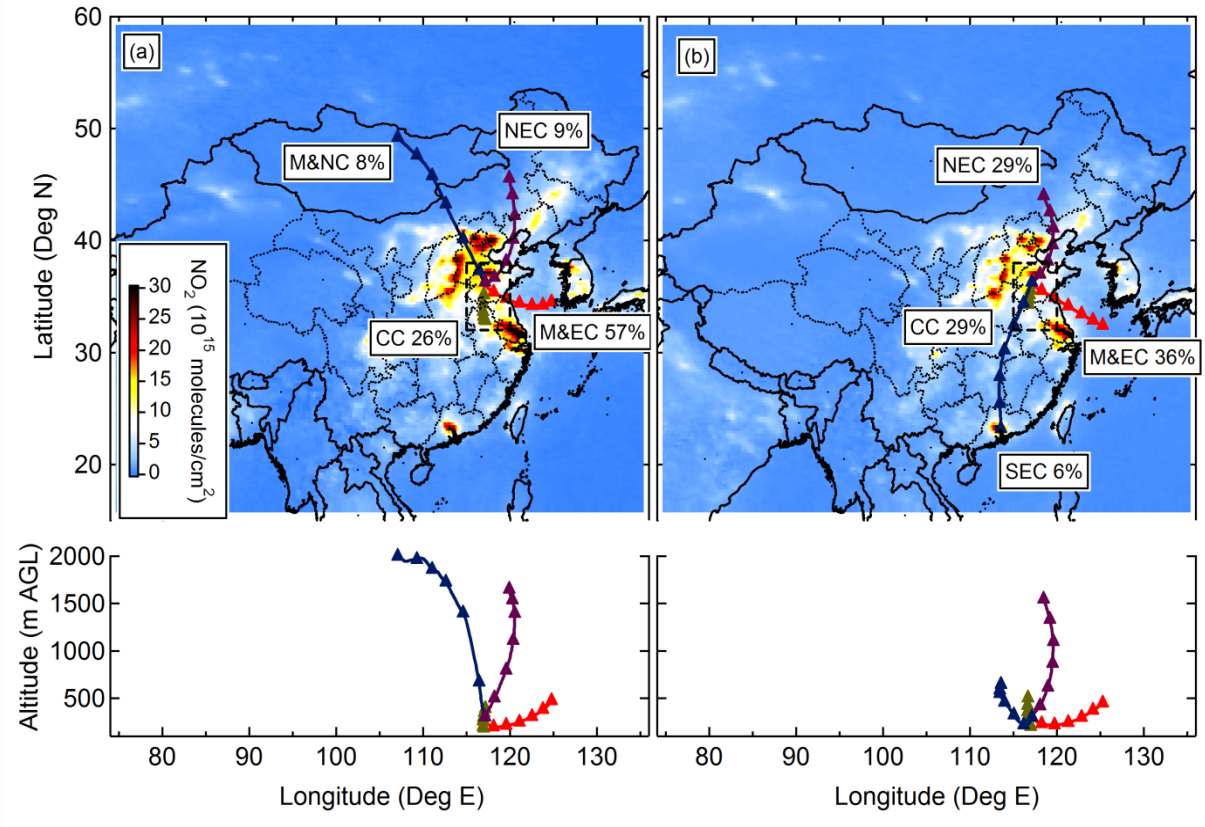


**Figure 5.** Climatological air mass transport pattern at Mt. Tai in (a) June and (b) July-August over 2003-2015. The maps are color-coded by the $NO_2$ column density retrieved from SCIAMACHY (2003-2011) and GOME-2 (B) (2013-2015). The box (dashed line) refers to the domain for which the satellite retrievals were averaged. Five major air masses: (1) M&EC: Marine and East China, (2) NEC: Northeast China, (3) CC: Central China, (4) SEC: Southeast China, (5) M&NC: Mongolia and North China.

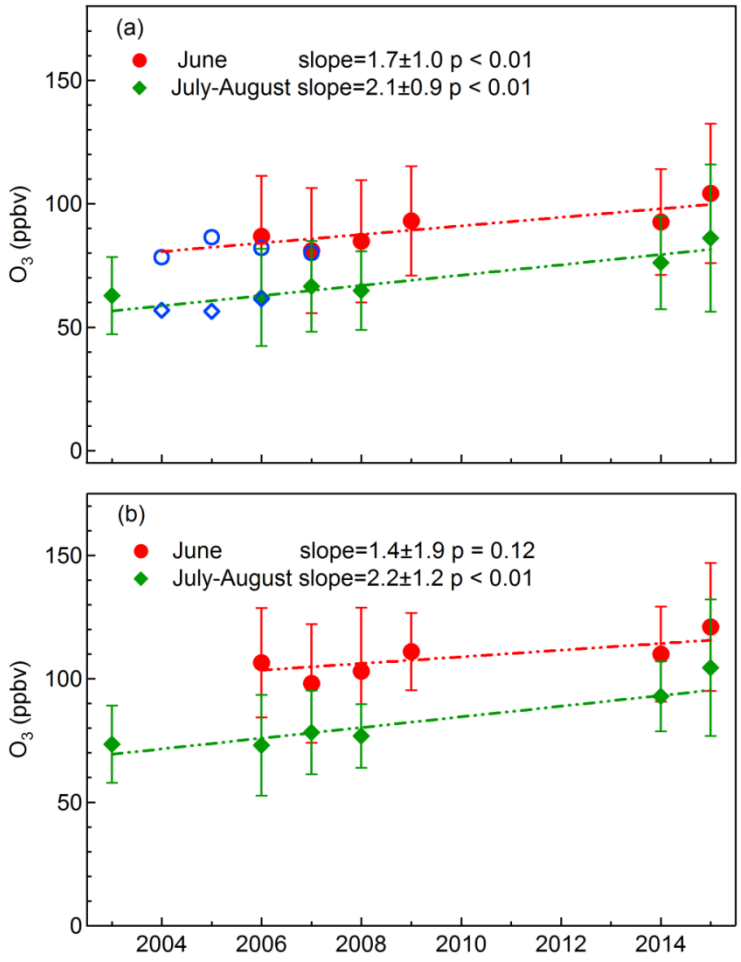


**Figure 6.** Monthly averaged (a) 1-hour and (b) MDA8 $O_3$ mixing ratios at Mt. Tai in June and July-August over 2003-2015. Error bars indicate the standard deviation of the mean. The blue open circles and squares represent the data taken from Kanaya et al. (2013). The fitted lines are derived from the least square linear regression analysis with the slopes (± 95% confidence intervals) and *p* values annotated.

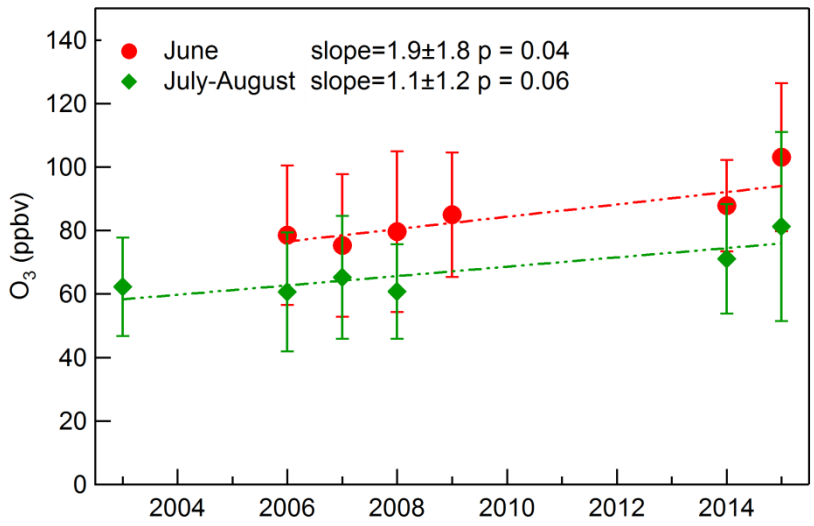


**Figure 7.** Monthly averaged nighttime $O_3$ mixing ratios (inferring the regional background $O_3$) at Mt. Tai in June and July-August over 2003-2015. Error bars indicate the standard deviation of the mean. The fitted lines are derived from the least square linear regression analysis with the slopes (± 95% confidence intervals) and *p* values annotated.

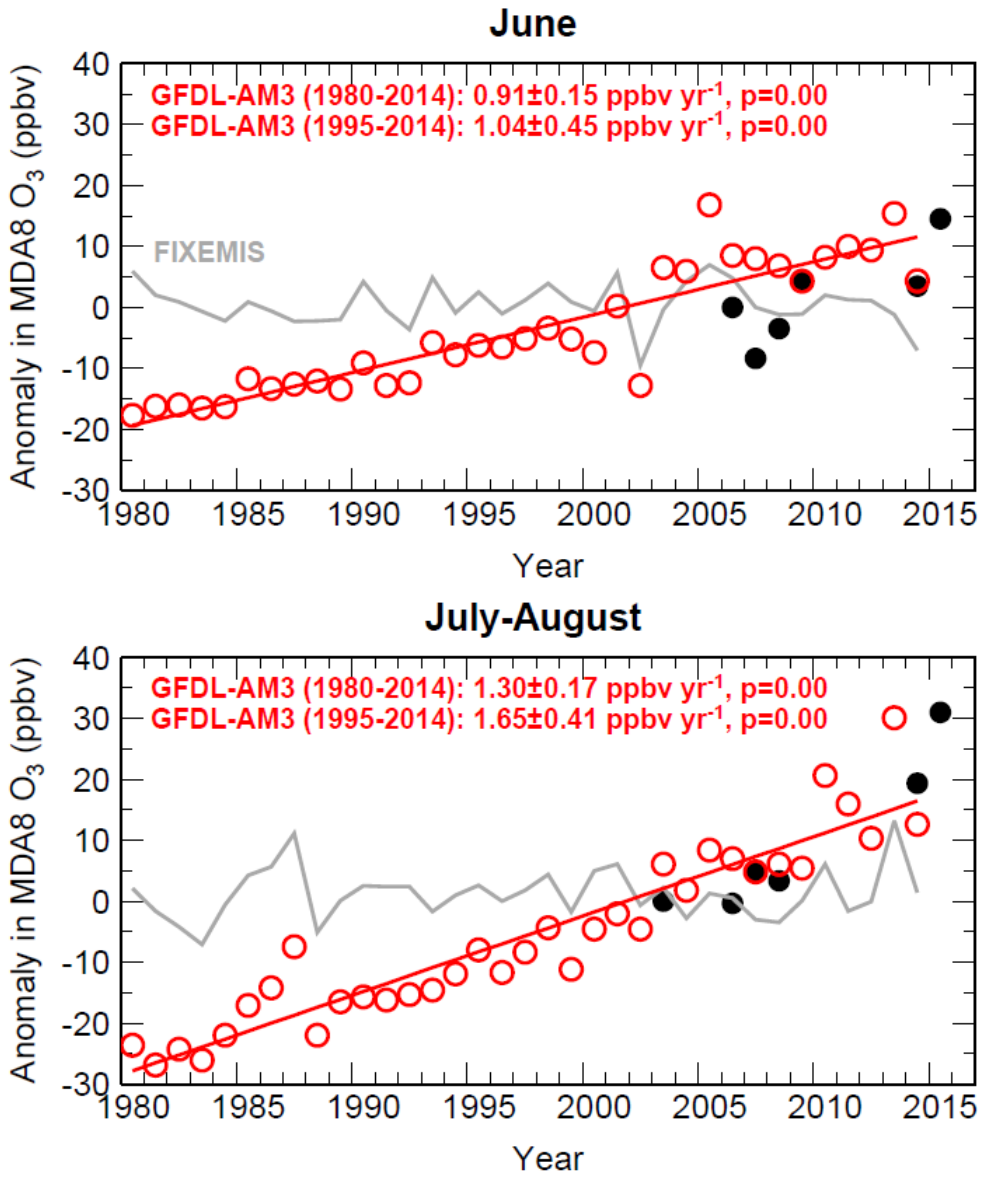


**Figure 8.** Comparison of ozone trends at Mt. Tai. (a) Anomalies in the June average of MDA8 $O_3$ from 1980 to 2015 as observed (black dots) and simulated by the GFDL-AM3 model with time-varying (red circles) and constant anthropogenic emissions (gray lines). (b) Same as (a) but for the July-August average. The model is sampled in the surface level. The linear trends over 1980-2014 and 1995-2014, including the 95% confidence limits and p-values, are shown.

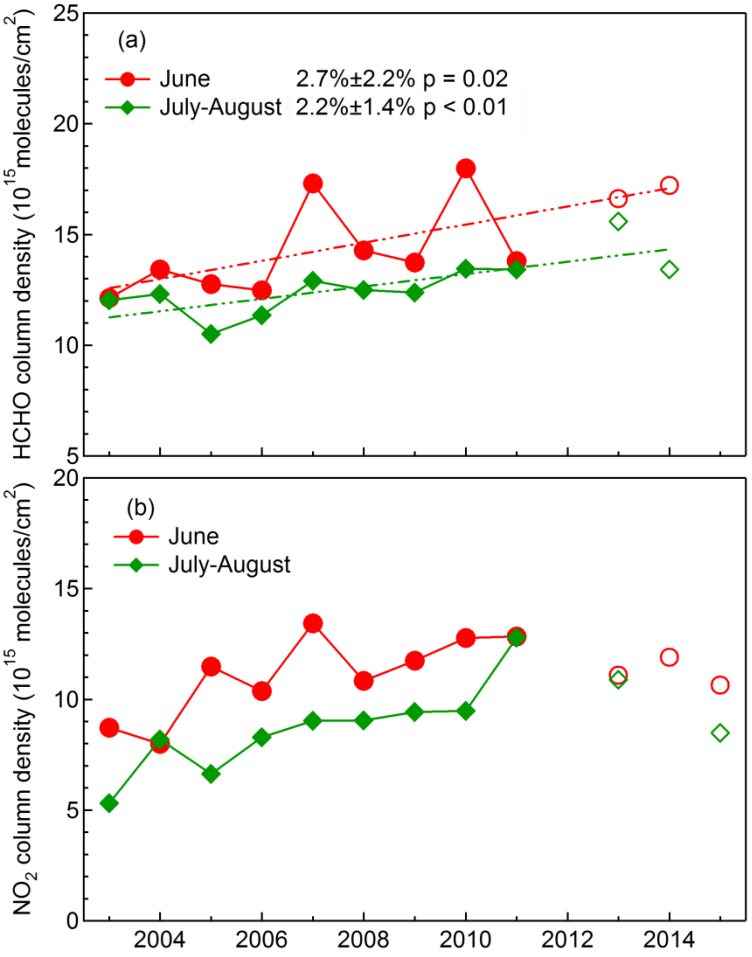


**Figure 9.** Monthly average column density of (a) formaldehyde and (b) $NO_2$ retrieved from SCIAMACHY (2003–2011; solid markers) and GOME-2 (B) (2013–2015; open markers) for the target domain (32 °–38 °N,115 °–120 °E). For formaldehyde, the fitted lines are derived from the least square linear regression analysis with the slopes (±95% confidence intervals) and *p* values also shown.

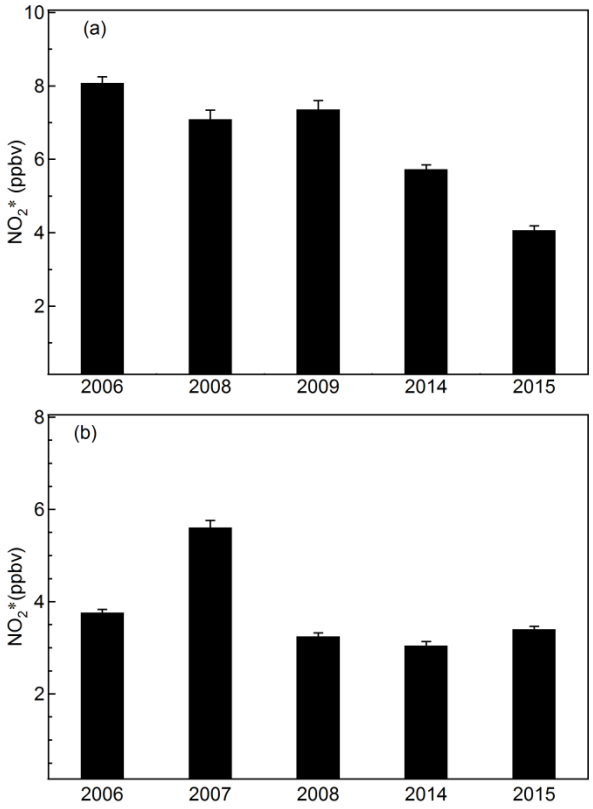


**Figure 10.** Monthly averaged $NO_2$* concentrations measured at Mt. Tai in (a) June and (b) July-August during 2006–2015. Error bars indicate the standard error of the mean. Note that the data point in June 2014 is for $NOx^*$ instead of $NO_2$*.

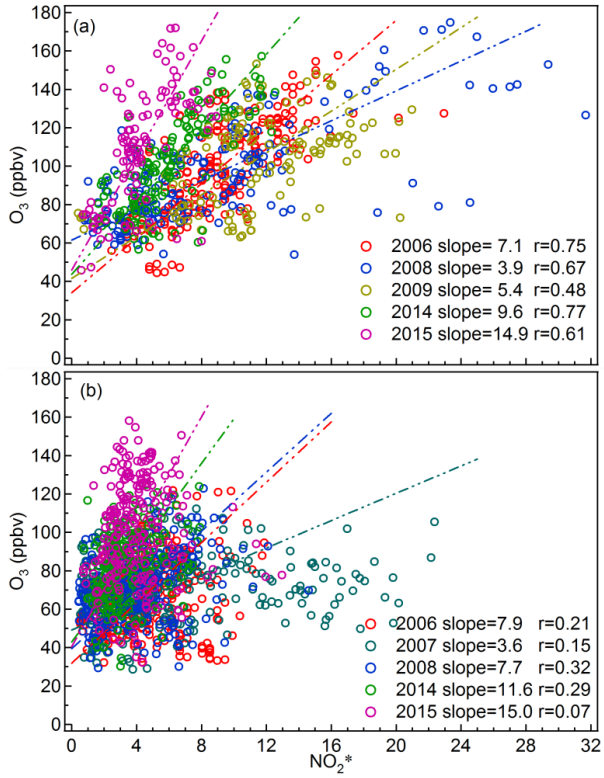


**Figure 11.** Scatter plots of $O_3$ versus $NO_2$* at Mt. Tai in (a) June and (b) July–August during 2006–2015. Only the afternoon data (i.e., 12:00-18:00 local time) were used for this analysis. Note that the $NO_2$* data in June 2014 stand for NOx* ($NO_x$*=NO+$NO_2$*), of which NO usually presents a minor fraction. The slopes are determined by the reduced major axis (RMA) method.